Electronic Supplementary Material

Colloidal Synthesis of Nanoparticles : from Bimetallic to High Entropy Alloys

Cora Moreira Da Silva,[*a] Hakim Amara,[a,b] Frédéric Fossard,[a] Armelle Girard, [a,c], Annick Loiseau,[a] and Vincent Huc[d]

[a] Laboratoire d'Etude des Microstructures, CNRS, ONERA, U. Paris-Saclay, Châtillon, 92322, France
[b] Université de Paris, Laboratoire Matériaux et Phénomènes Quantiques (MPQ), CNRS-UMR7162, 75013 Paris, France
[c] Université Versailles Saint-Quentin, U. Paris-Saclay, Versailles, 78035, France
[d] Institut de Chimie Moléculaire et des Matériaux d'Orsay, CNRS, Paris Sud, U. Paris-Saclay, Orsay, 91045, France

In this Supplementary Material, different analyses are presented to show inambiguously the structure of synthesized HEA NPs. Thus for all the syntheses discussed in the manuscript, large area HAADF STEM images are shown as well as the diameter distribution histograms to prove the successful production of non-aggregated NPs with a particularly well controlled diameter. Electron diffraction patterns are also displayed and analysed to prove the fcc structure of the NPs. To highlight the chemical compositions of the NPs, EDX spectra on region containing many NPs are depicted and also EDX quantifications over several dozen of isolated NPs.

1. Bimetallic alloys

Fe-Pt nanoparticles

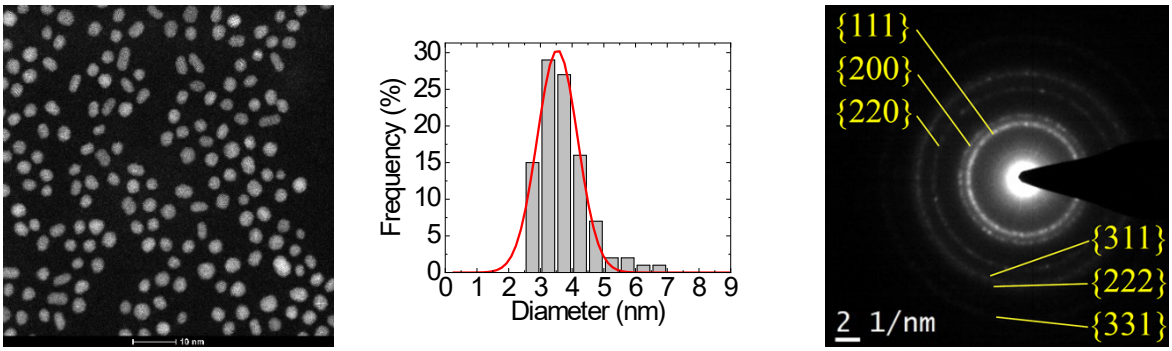

(a) (b) (c)

Fig. S1: (a) Large area HAADF STEM image including a large amount of NPs showing the monodispersity and non-aggregation. (b) Diameter distribution histogram obtained on 500 particles counted by ImageJ software, giving d = (3.5 ± 1.3) nm. (c) Electron diffraction pattern showing a fcc structure with planes: {111}, {200}, {220}, {311}, {222}, {331} and the deduced lattice parameter a = (0.400 ± 0.003) nm

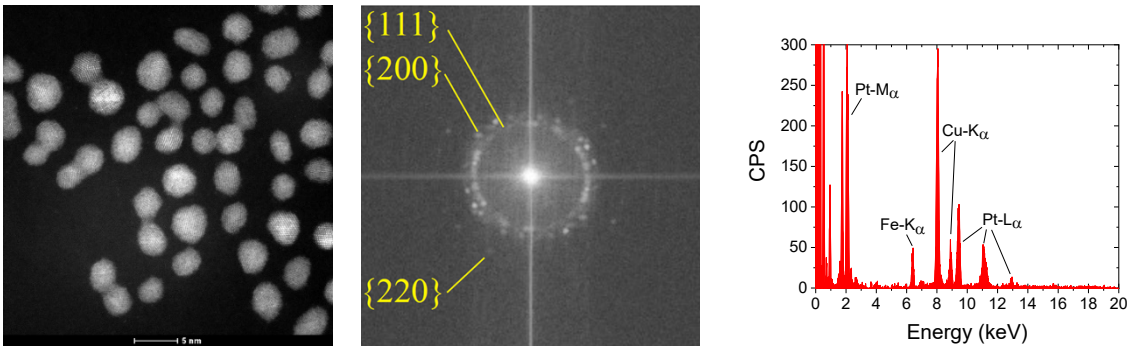

(a) (b) (c)

Fig. S2: (a) HAADF UHR-STEM image showing crystallographic planes, (b) its FFT showing the planes: {111}, {200} and {220}, confirming the results obtained in Fig. S1 and (c) EDX spectrum obtained on Fe-Pt sample giving the average composition: Fe = 48 %at. and Pt = 52 %at. Cu-K_α signals are due to the copper TEM grid.

NPs	Fe (%at.)	Pt (%at)
1	44.41	55.59
2	51.89	48.11
3	34.86	65.14
4	50.77	49.23
5	57.44	42.56
6	52.74	47.26
7	40.28	59.72
8	54.36	45.64
9	42.37	57.63
10	22.70	77.30
11	41.95	58.05
12	46.22	53.78
13	37.52	62.48
14	48.75	51.25
15	49.99	50.01
16	25.88	74.12
17	48.93	51.07

18	41.87	58.13
19	59.73	40.27
20	42.82	57.18
21	49.57	50.43
22	48.01	51.99
23	52.25	47.75
24	46.32	53.68
25	54.82	45.18
26	37.70	62.30
27	30.64	69.36
28	32.56	67.44
29	51.36	48.64
Mean	**44.78**	**55.22**
Sigma	**9.19**	**9.19**

Table S1: Table listing the EDX quantification (%at.) of each isolated particle shown in the Figure 3b of article, from which the chemical composition and the deviation from the chemical composition was determined.

2. Beyond bimetallic alloys

First Co-Ni-Pt nanoparticles synthesized at 280°C

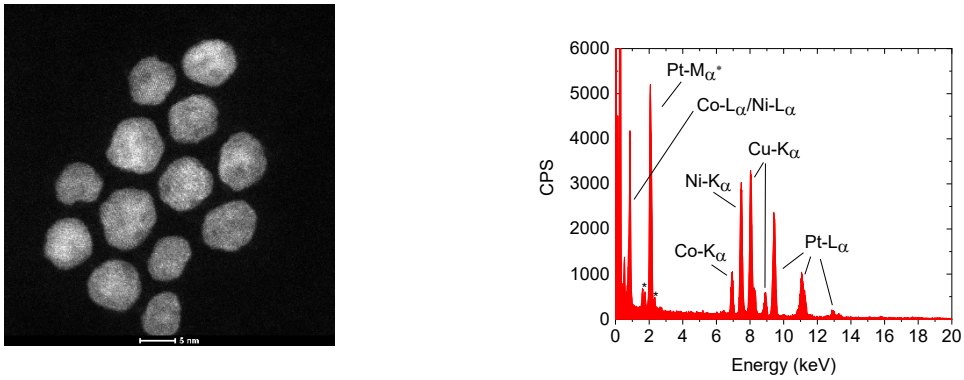

(a) (b)

Fig. S3: (a) HAADF UHR-STEM image of NPs. (b) EDX spectrum obtained on Co-Ni-Pt synthesized at 280 °C, giving the average composition: Co = 8 %at., Ni = 54 %at. and Pt = 37 %at. Cu-K_α signals are due to the copper TEM grid.

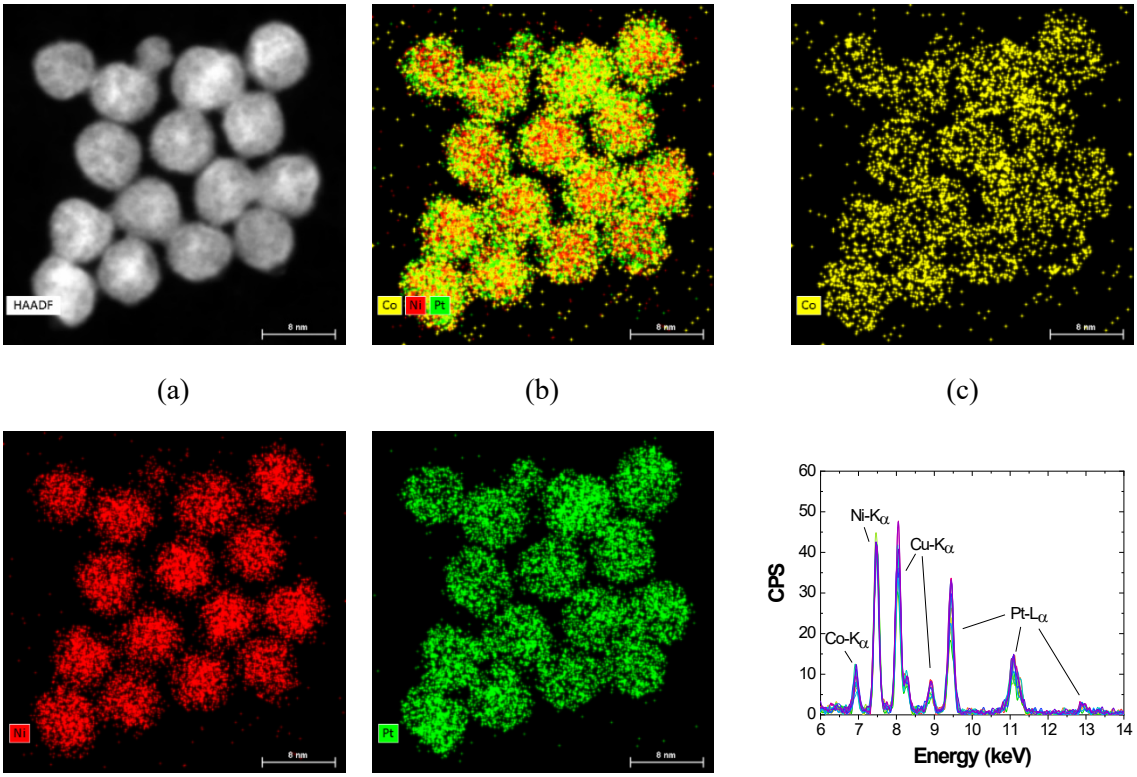

(a) (b) (c)

(c) (d) (e)

Fig. S4: (a) HAADF STEM image of CoNiPt NPs synthesized at 280 °C, with EDX chemical mapping: (b) superposition of all signals, (c) Co (K_α line), (d) Ni (K_α line) and (d) Pt (L_α line) showing the spatial correlation between the different elements. (e) Superposition of each isolated NPs spectra presented in Fig. S5 showing the chemical composition uniformity between of NPs (the spectra are smoothed by the Savitzky-Golay method on 5 points with the OriginPro 2018 software to reduce noise and improve observation).

NPs	Co (%at.)	Ni (%at.)	Pt (%at.)
1	8.09	58.36	33.55
2	10.88	42.79	46.33
3	7.58	51.81	40.61
4	9.29	53.13	37.58
5	8.09	58.74	33.17
6	8.91	61.18	29.91
7	8.98	61.65	29.37
8	5.64	59.08	35.28
9	10.61	51.43	37.96
10	5.16	53.2	41.64
11	7.09	59.55	33.36
12	11.18	49.58	39.24
13	8.4	52.47	39.13
14	7.55	49.68	42.77
Mean	**8.39**	**54.48**	**37.14**
Sigma	**1.79**	**5.44**	**4.93**

Table S2: Table listing the EDX quantification (%at.) of each isolated particle shown in the Figure S5, from which the chemical composition and the deviation from the chemical composition was determined.

Second Co-Ni-Pt nanoparticles synthesized at 290°C

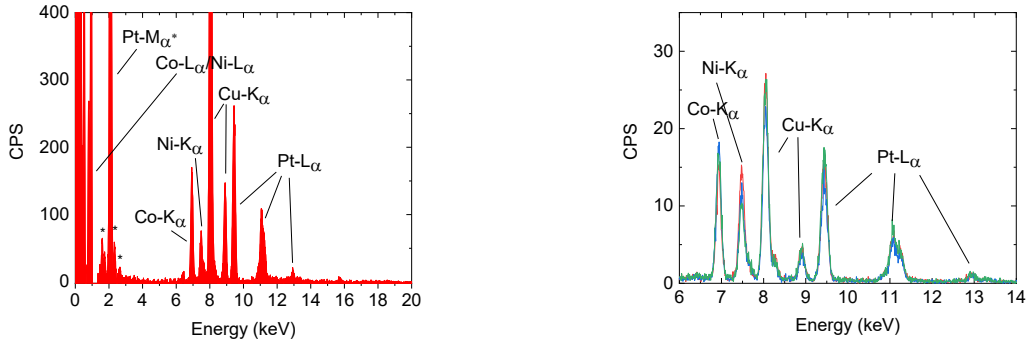

Fig. S5: EDX spectrum obtained on Co-Ni-Pt synthesized at 290 °C, giving the composition : Co = 32 %at., Ni = 23 %at. and Pt = 45 %at. No contamination is noted. (b) Superposition of each isolated NPs spectra showing the chemical composition uniformity between NPs (the spectra are smoothed by the Savitzky-Golay method on 5 points with the OriginPro 2018 software to reduce noise and improve observation). Cu-K_α signals are due to the copper TEM grid.

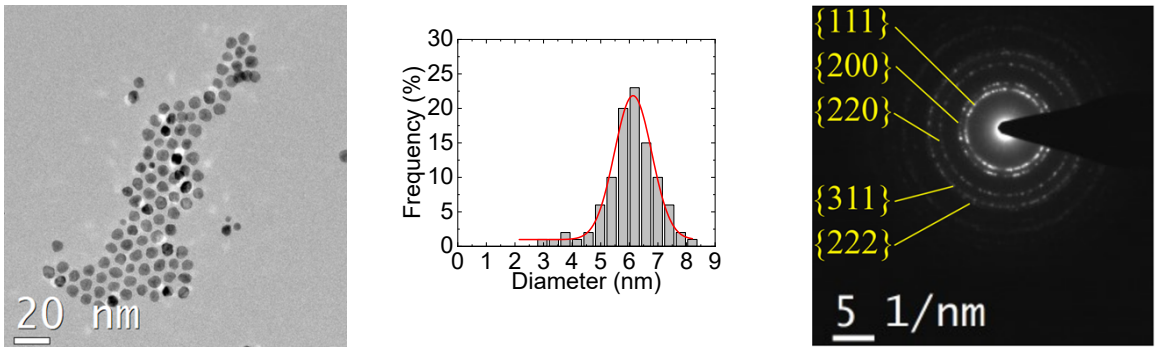

Fig. S6: (a) TEM image showing the monodispersity and the non-aggregation of the particles. (b) Size distribution histograms obtained on 500 particles, giving d = (6.1 ± 1.3) nm. (c) Electron diffraction pattern showing a fcc structure ({111}, {200}, {220}, {311}, {222}) and the deduced lattice parameter a = (0.370 ± 0.005) nm

First Fe-Co-Ni-Pt nanoparticles

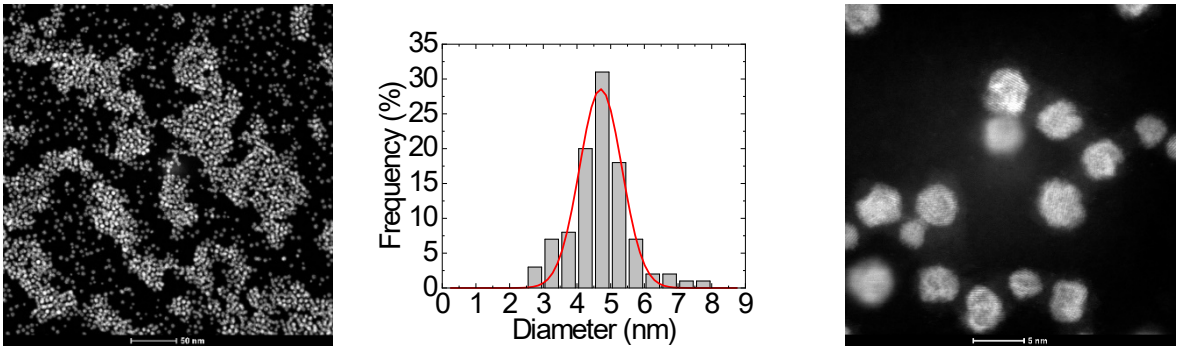

(a) (b) (c)

Fig. S7: (a) Large area HAADF STEM image containing a large amount of NPs showing the monodispersity and the non-aggregation of the particles. (b) Diameter distribution histogram obtained on 500 particles, giving d = (4.7 ± 1.3) nm. (c) HAADF UHR-STEM image of NPs.

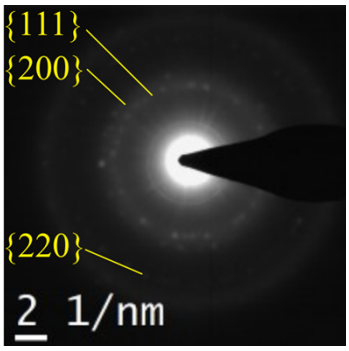

Fig. S8: Electron diffraction pattern showing a fcc structure ({111}, {200}, {220}, {311}) and the deduced lattice parameter a = (0.370 ± 0.005) nm

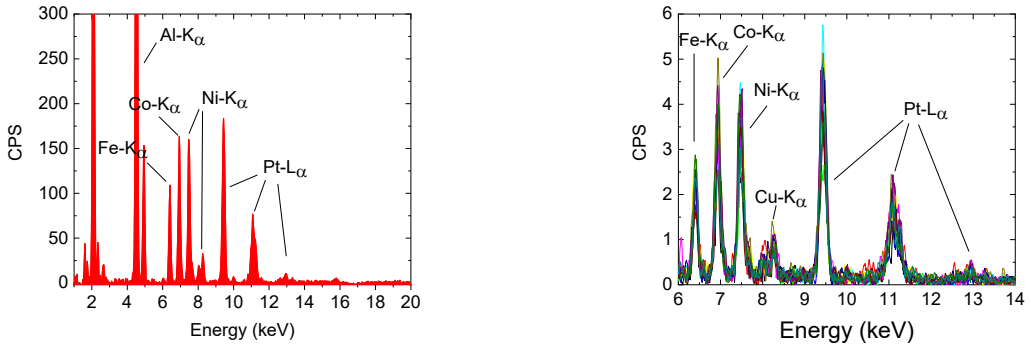

(a) (b)

Fig. S9: (a) EDX spectrum obtained on a first Fe-Co-Ni-Pt sample giving the averaged composition: Co = 22 %at., Fe = 14 %at., Ni = 27 %at. and Pt = 37 %at. Al-K signals are due to the aluminum TEM grid. (b) Spectra superposition of various isolated Fe-Co-Ni-Pt NPs showing the chemical composition uniformity between NPs (the spectra are smoothed by the Savitzky-Golay method on 5 points with the OriginPro 2018 software to reduce noise and improve observation).

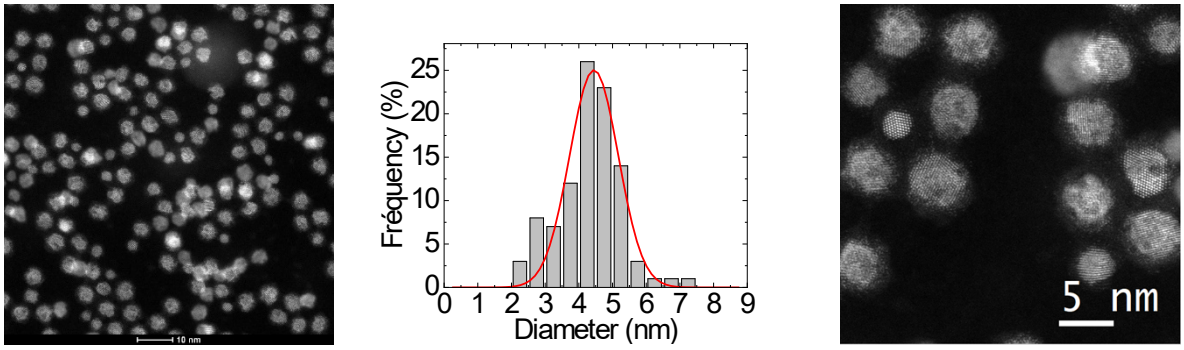

(a) (b) (c)

Fig. S10: (a) Large area HAADF STEM image covering containing a large amount of NPs showing the monodispersity and the non-aggregration of the particles. (b) Size distribution histograms obtained on 500 particles, giving d = (4.4 ± 0.9) nm. (c) HAADF UHR-STEM image of NPs.

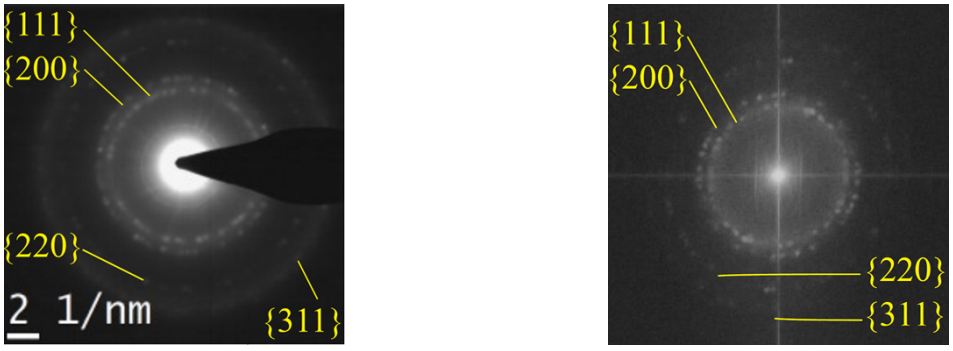

(a) (b)

Fig. S11: The NPs crystallinity demonstrated by crossed techniques: (a) diffraction electron pattern obtained on large quantity of particles showing the planes : {111}, {200}, {220} and {311}. (b) FFT of HAADF HR-STEM image in Fig. S13 showing crystallographic planes and (c) its FFT showing the planes: {111}, {200}, {220} and {311}. The lattice parameter deduced is a = (0.371 ± 0.002) nm

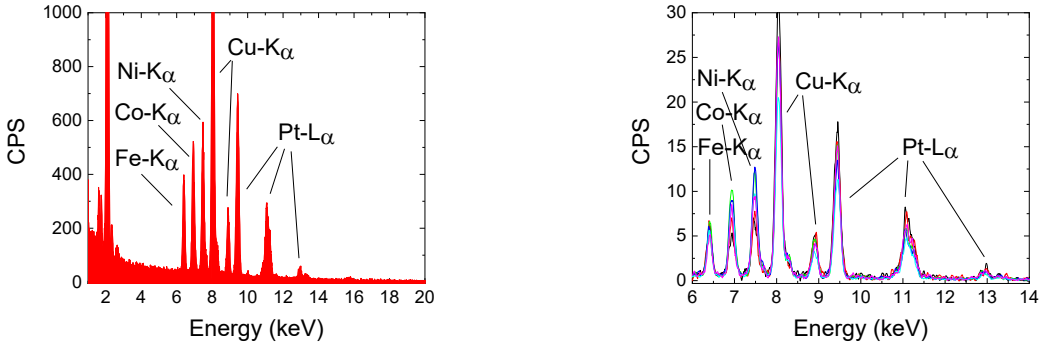

Fig. S12: EDX spectrum obtained on a second Fe-Co-Ni-Pt sample, giving the composition: Co = 19 %at., Fe = 12 %at., Ni = 26 %at. and Pt = 43 %at. (b) Spectra superposition of various isolated Fe-Co-Ni-Pt NPs showing the chemical composition uniformity between NPs (the spectra are smoothed by the Savitzky-Golay method on 5 points with the OriginPro 2018 software to reduce noise and improve observation). Cu-K_α signals are due to the copper TEM grid.

Fe-Co-Ni-Pt-Ru nanoparticles

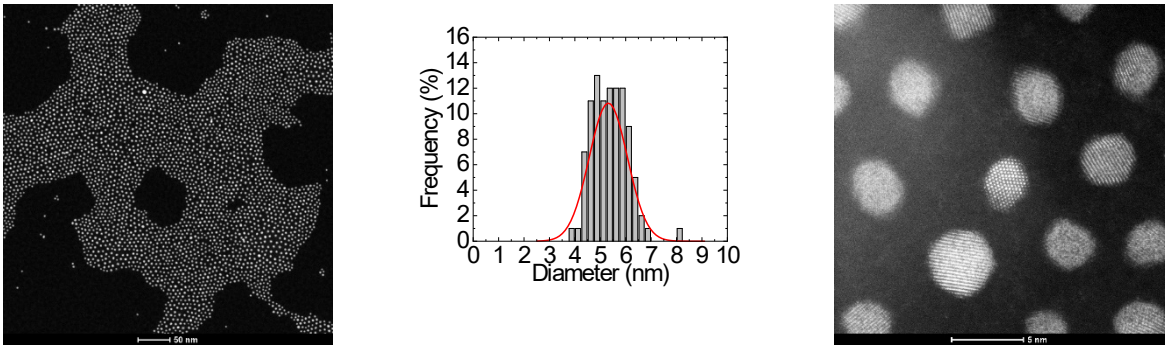

(a) (b) (c)

Fig. S13: (a) Large area HAADF STEM image including a large amount of NPs showing the monodispersity and the non-aggregation of the particles. (b) Size distribution histograms obtained on 500 particles, giving d = (5.3 ± 1.5) nm. (c) HAADF UHR-STEM image of NPs.

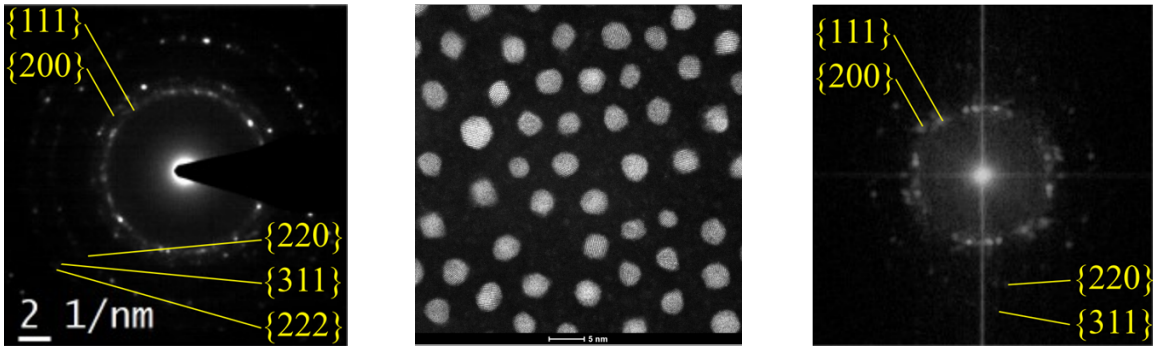

(a) (b) (c)

Fig. S14: NPs crystallinity demonstrated by crossed techniques : (a) diffraction electron pattern obtained on large quantity of particles showing the planes : {111}, {200}, {220}, {311}, {222} and {400}. (b) HAADF HR-STEM image showing crystallographic planes and (c) its FFT showing the planes: {111}, {200}, {220} and {311}. The deduced structure is fcc with a = (0.370 ± 0.003) nm

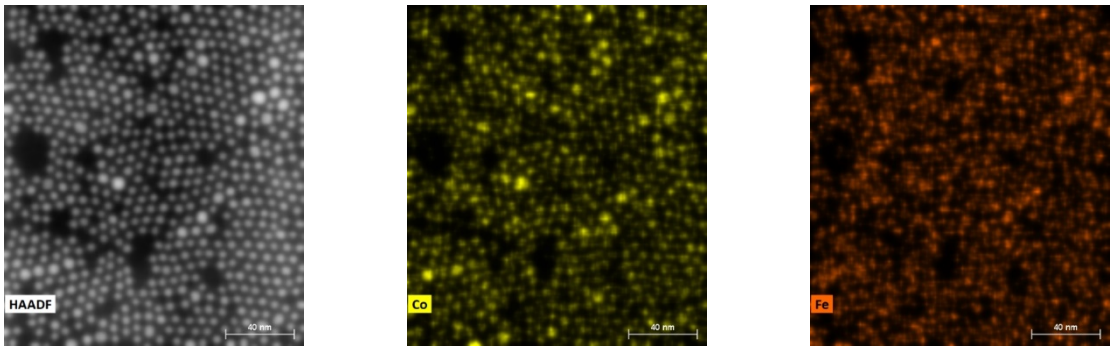

(a) (b) (c)

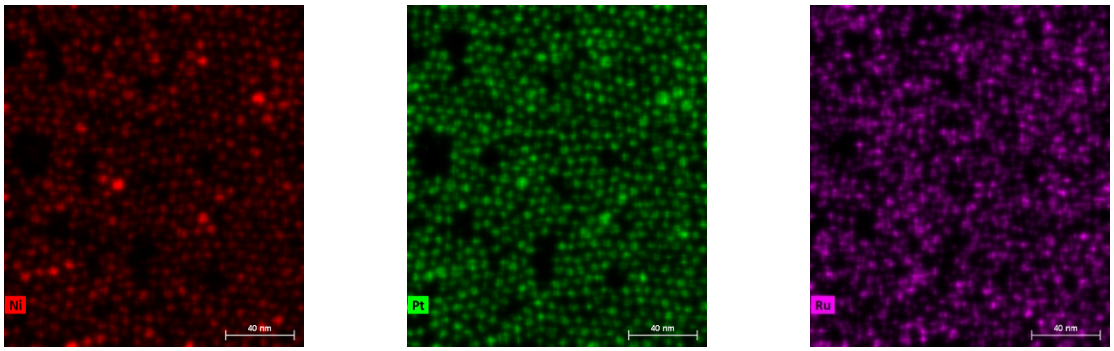

(d) (e) (f)

Fig. S15: (a) HAADF-STEM images and EDX chemical mapping of (b) Co (K_α line), (c) Fe (K_α line), (d) Ni (K_α line), (e) Pt (L_α line), (f) Ru (K_α line) showing the spatial correlation between the different elements present in individual FeCoNiPtRu NPS on a large area of the sample presented in Fig. 6.

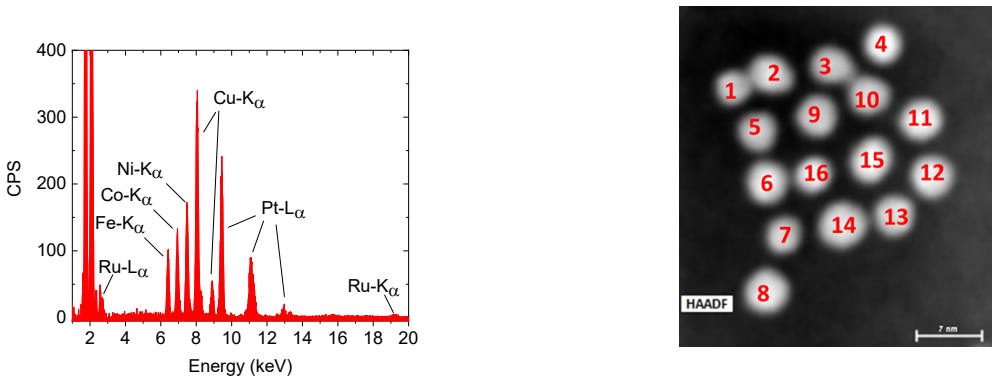

(a) (b)

Fig. S16: EDX spectrum obtained in the same area giving the composition : Co = 24 %at., Fe = 13 %at., Ni = 24 %at., Pt = 34 %at. and Ru = 5 %at. Cu-K_α signals are due to the copper TEM grid. (b) HAADF-STEM image of Fig. 6 on which a chemical quantification on each isolated NP was done, the results are listed in Table S3

NPs	Fe (%at.)	Co (%at.)	Ni (%at.)	Ru (%at.)	Pt (%at.)
1	15,06	20,19	21,5	1,45	41,8
2	13,74	21,98	24,63	5,31	34,34
3	13,26	22,14	25,16	4,34	35,1
4	14,51	18,28	22,63	5,15	39,43
5	12,95	21,12	24,61	5,14	36,18
6	12,82	21,72	27,73	1,58	36,15
7	11,89	24,66	23,2	1,58	38,67
8	11,84	20,34	22,26	7,8	37,76
9	9,51	24,64	23,17	5,3	37,38
10	11,4	22,01	24,01	5,7	36,88
11	11,42	21,4	25,77	4,14	37,27
12	10,84	18,57	22,76	10,65	37,18
13	11,37	22,18	18,6	7,99	39,86
14	12,73	24,19	22,49	7,6	32,99
15	9,75	24,34	22,89	5,58	37,44
16	9,23	19,16	22,45	9,75	39,41
Mean	**12,02**	**21,68**	**23,37**	**5,57**	**37,37**
Sigma	**1,71**	**2,06**	**2,03**	**2,72**	**2,20**

Table S3: Chemical composition distribution extracted from EDX chemical mapping recorded on isolated particles presented in Fig. 6 and S18.